1-1-2013

The nanostructure of three-dimensional scaffolds enhances the current density of microbial bioelectrochemical systems

Victoria Flexer
University of Queensland

Jun Chen
University of Wollongong, junc@uow.edu.au

Bogdan C. Donose
University of Queensland

Peter C. Sherrell
University of Wollongong, psherrel@uow.edu.au

Gordon G. Wallace
University of Wollongong, gwallace@uow.edu.au

See next page for additional authors

The nanostructure of three-dimensional scaffolds enhances the current density of microbial bioelectrochemical systems

Abstract

Bioelectrochemical systems encompass a range of electrochemical systems wherein microorganisms are used as biocatalysts. These range from classical microbial fuel cells to novel microbial electrosynthesis processes. The future of practical applications relies on increased performance. In all cases the development of new electrode materials is essential to overcome the low current densities of bioelectrochemical systems. Here we describe a new biocompatible, highly conductive three-dimensional scaffold electrode, NanoWeb-RVC, with a hierarchical porous structure, synthesized by direct growth of carbon nanotubes on a macroporous substrate. The nanostructure of these electrodes enhances the rate of bacterial extracellular electron transfer while the macrostructure ensures efficient mass transfer to and from the electrode surface. NanoWeb-RVC electrodes showed a current density of (6.8 ± 0.3) mA cm-2, almost three times higher than a control electrode with the same macroporous structure but lacking the nanostructure. This current density is among the highest reported to date for a microbial bioanode.

Keywords

systems, scaffolds, bioelectrochemical, microbial, density, nanostructure, three, current, dimensional, enhances

Disciplines

Engineering | Physical Sciences and Mathematics

Publication Details

Flexer, V., Chen, J., Donose, B. C., Sherrell, P. C., Wallace, G. G. & Keller, J. (2013). The nanostructure of three-dimensional scaffolds enhances the current density of microbial bioelectrochemical systems. Energy and Environmental Science, 6 (4), 1291-1298.

Authors

Victoria Flexer, Jun Chen, Bogdan C. Donose, Peter C. Sherrell, Gordon G. Wallace, and Jurg Keller

The nanostructure of three-dimensional scaffolds enhances the current density of microbial bioelectrochemical systems

Victoria Flexer[*,1], *Jun Chen*[2], *Bogdan C. Donose*[1], *Peter Sherrell*[2], *Gordon G. Wallace*[2], *Jurg Keller*[1]

1- The University of Queensland, Advanced Water Management Centre, Level 4, Gehrmann Building (60), Brisbane, QLD 4072, Australia

2- ARC Centre of Excellence for Electromaterials Science, Intelligent Polymer Research Institute, AIIM Facility, Innovation Campus, University of Wollongong, NSW, 2522, Australia

ABSTRACT. Bioelectrochemical systems encompass a range of electrochemical systems wherein microorganisms are used as biocatalysts. These range from classical microbial fuel cells to novel microbial electrosynthesis processes. The future of practical applications relies on increased performance. In all cases the development of new electrode materials is essential to overcome the low current densities of bioelectrochemical systems. Here we describe a new biocompatible, highly conductive three-dimensional scaffold electrode, NanoWeb-RVC, with a hierarchical porous structure, synthetised by direct growth of carbon nanotubes on a macroporous substrate. The nanostructure of these electrodes enhances the rate of bacterial extracellular electron transfer while the macrostructure ensures efficient mass transfer to and from the electrode surface. NanoWeb-RVC electrodes showed a current density of (6.8 ± 0.3) mA cm^{-2}, almost three times higher than a control electrode with the same macroporous structure but lacking the nanostructure. This current density is among the highest reported to date for a microbial bioanode.

Introduction

In microbial bioelectrochemical systems, whole cells are used as biocatalysts to catalyse oxidation and/or reduction reactions.[1-4] Microbial fuel cells are the classical and more widely studied example of bioelectrochemical systems, performing the double task of wastewater treatment and electricity generation. In a typical microbial fuel cell, the anode is used to harvest electrons from wastewater while oxidising organic pollutants. More recently, the concept has been extended to the possibility of generating higher value products than electricity.[5] In microbial electrolysis cells, electrons are used as reducing power at the cathode to drive the microbial metabolism and create valuable products.[5]

The viability of prospective applications of microbial bioelectrochemical systems is highly dependent on performance improvements, particularly increased electrical currents.[6-8] Current production is dependent on the microbial consortia, bioelectrochemical reactor design, and electrode materials, among other factors.[8] While the first two key characteristics have been widely researched for more than a decade, until very recently, most of the work on bioelectrochemical systems used only commercially available carbonaceous materials,[1, 9, 10] such as carbon felt, carbon cloth, carbon paper, graphite granules or rods, etc. Synthesis and design of new electrode materials, purposely built with bioelectrochemical applications in mind is only very recent.[6, 11-21] The classical approach in research on prospective electrode materials aims at increasing the active surface area available for biofilm growth. On the other hand, another strategy aims at designing materials with specific properties that will improve the bacteria-electrode interaction, especially the rate of electron transfer, to enhance the activity of the biofilms.

It has already been predicted that a current increase beyond 1 mA cm^{-2} will be limited by the transfer of substrate and the removal of H^+ at flat electrodes.[22-24] In this category, we also include rough electrodes, *i.e.* electrodes with roughness features below the micron scale.

Therefore, it would be a great advantage if three-dimensional anodes and cathodes could be employed for the construction of bioelectrochemical systems, as it is already common practice for classical fuel cells. Here, we refer to true three-dimensional electrodes, where all three geometric dimensions are of the same order of magnitude, and where bacteria will be able to develop in the interior of the three-dimensional structure, as opposed to rough electrode surfaces or dense fibrous material such as carbon felt. Considering the predicted mass-transfer limits mentioned above, these new three-dimensional materials should bear macropores at least in the tens of micrometre scale that would allow for efficient mass transport. Ideally, electrodes should bear multidirectional pores, to maximise fluid flow towards and out of the pores.[25, 26]

In addition to ensuring efficient mass transfer to and from the electrode surface, the macroporosity will drastically increase the accessible surface area of the electrode and therefore the microbial loading level, allowing for a maximization of the current. Reticulated vitreous carbon (RVC) is a commercially available cheap material composed solely of vitreous carbon. It is an open-pore foam material of honeycomb structure, with an exceptionally high void volume (between 90 and 97% depending on porosity, defined as pores per inch, ppi). RVC shows all the intrinsic properties of vitreous carbon, most notably for our application, high electrical conductivity.[27] It has been extensively used in the field of electrochemistry, though not very often in microbial bioelectrochemical systems.[9, 28, 29]

Carbon nanotubes (CNT), having a high electroactive surface area, extremely high conductivity and useful mechanical properties,[30] are very promising candidates to be incorporated into microbial bioelectrochemical devices. Recently, several authors have reported the coating of different scaffold materials with carbon nanotube inks and produced promising current densities.[14-18, 31] In an innovative approach to avoid the need of coating surfaces with CNT, a new method was recently developed to directly grow carbon nanotube

networks on any type of substrate. This is achieved by modifying the generally employed route of chemical vapour deposition (CVD) synthesis.[30, 32] The so called CNT NanoWeb comprises entangled multi-wall carbon nanotubes integrated onto an underlying conductive carbon layer.[30, 32]

Here we report on a new prospective microbial electrode material bearing a hierarchical porous structure, NanoWeb-RVC, where CNT NanoWeb were directly grown on a reticulated vitreous carbon (RVC) scaffold. The results show that the new electrode material combines the advantages of both CNT NanoWeb and an open three-dimensional scaffold. The biofilm is formed on top of the CNT texture structure. The improved bioanode performance suggests that the CNT NanoWeb not only improves the bacterial attachment to the electrode surface but also enhances the extracellular electron transfer.

Results and discussion

In figure 1, we can see that the SEM images of the NanoWeb-RVC electrode mirror the macroporous pure RVC structure. The NanoWeb appears as a fine "fur" or roughness on the surface, in clear contrast to the flat unmodified RVC. It clearly shows the CNT NanoWeb had been successfully deposited onto the RVC surface without damaging its original macroporous structure, which is critical for the subsequent biofilm formation. The high magnification SEM image of the grown NanoWeb surface shows an entangled array of fine carbon nanotubes with an average diameter of about 60 nm. In addition, photographic images of RVC before and after the CNT NanoWeb modification also demonstrate the clearly visible colour change from silver-black (pure RVC, showing the characteristic glow of vitreous carbon) to dark-black (NanoWeb modified RVC). Raman spectroscopy of the NanoWeb showed typical peaks at 1325 cm^{-1} and 1588 cm^{-1} (respectively D band and G band), indicating that the top

tangled array structure consists of multi-walled carbon nanotubes (see Figure S1 in Supporting Information).

The thick line in Figure 2 shows the catalytic current development from time of inoculation with anodic effluent from an existing BES reactor for a NanoWeb-RVC electrode. The electrode's geometrical dimensions are (10 x 10 x 6.6) mm thick, *i.e.* a true three-dimensional electrode as previously defined. Experiments were run at room temperature, with acetate as the sole organic feed source. The reported current values have been normalized by the projected surface area of the electrode (1 cm^2 footprint). Experiments were carried out under very mild magnetic stirring of the solution, with no direct forced flow through the electrode. Catalytic current started to develop after 4 days. After 7 days, the magnetic stirring rate in the reactor was increased from 100 RPM to 250 RPM, which translated in a much faster current increase. After 11 days, the current appeared to have reached a stationary value, but when the magnetic stirring was accelerated again (to 500 RPM) the current continued to increase. 36 hours later, the current seemed to stabilize again. We increased the magnetic stirring once more, but the signal became too noisy and the stirring rate was reduced to 300 RPM. The current remained almost constant for 3 days, and then it sharply decreased due to substrate depletion in the batch reactor. The current picked up again quickly after the media was replaced with fresh anolyte. The catalytic current reached a maximum of 6.8 mA cm^{-2}. This value translates to 10.3 mA cm^{-3}, when normalized to the electrode volume. This high current density was reproduced in an independent second run, *i.e.* a new electrode was studied with new inoculum in the same reactor after completion of the first experiment. The maximum current density was within 5% of that shown in Figure 2, though the current development profile was somewhat different, which is not uncommon for mixed-culture microbial systems.

We also performed analogous experiments with a control material. We used bare reticulated vitreous carbon (RVC), without the carbon nanotube or any other modifications. The current vs. time profile shown in Figure 2 (thin line) is similar to that of NanoWeb-RVC, though of much lower magnitude. The experiment took slightly longer to arrive to the maximum catalytic current, which was nearly three times lower than the corresponding maximal current of the NanoWeb RVC.

At the end of the chronoamperometry experiment, the RVC-NanoWeb electrode showed a distinctive reddish colour throughout, see Figure 3A. This is attributed to the uniform biofilm coverage and suggests the presence of cytochromes. When the electrode was broken into several pieces, the reddish colour was observed as well in the interior of the electrode sample, indicating that the biofilm had developed both on the outside and the inside of the three-dimensional scaffold. SEM images of the outside or the inside of the three-dimensional scaffold are almost identical, all of them showing consistent and uniform biofilm development. Figures 3B to 3D show images of the biofilm developed at the interior of the three-dimensional scaffold. Figure 3B and 3C show that the biofilm covers the entire available electrode surface, generating a thick and continuous biofilm. The biofilm is covering the electrode surface without clogging the pores, *i.e.* maintaining the open structure that is needed to achieve good mass transfer between the liquid and the biofilm/electrode. Figure 3D is an image of a partially broken and lifted biofilm, while Figure 3E shows a broken arm of the scaffold where we can distinguish the backbone of the RVC, the NanoWeb structure, and the biofilm. In Figure 3F individual microbial shapes can be distinguished. These appear to be rod-shaped and approximately 1 μm long. These individual microbial shapes are very similar to *Geobacterae sp.*, which are known to be rod-shaped bacteria, approximately 1 μm in length. *Geobacterae sp.* are also known to be rich in cytochromes. Therefore, these features might indicate an abundance of these bacteria in the electroactive

biofilms. This is consistent with previous data, which showed that these microorganisms are abundant in the mixed-culture anodic effluent used to inoculate our reactors.[33] We have to admit, however, that at this point this data is only indicative of the presence of such bacteria and cytochromes and that more detailed analysis would be needed to confirm this hypothesis.

At day 14 of the chronoamperometry experiment, after the maximum current had been reached, the chronoamperometry experiment was stopped to record a cyclic voltammogram in turnover conditions. This is shown in Figure 4 (thick line). The voltammogram exhibits the classic sigmoidal shape of electroactive biofilms under turnover conditions with very little hysteresis. The current starts to increase above -0.45 V and reaches a maximum around -0.1 V. All potentials in this manuscript are referred to the Ag/AgCl (saturated Cl^-) reference electrode. The plateau current is almost the same as the maximum current recorded in the chronoamperometry experiment. A first derivative analysis (shown in Figure S2 in Supporting Information) shows a symmetrical peak centred at -0.3 V (E_{hw}). The onset potential for the turnover CV and the value of E_{hw}, together with the strong red colour of our electrodes, suggest once again that cytochromes are involved in the electron transfer from bacteria to electrode.

At the end of the chronoamperometry experiment, the media in the reactor was replaced with fresh media without substrate. After 24h of an applied potential in the absence of substrate, cyclic voltammogram experiments were recorded in non-turnover conditions and this is shown in the inset of Figure 4. A broad peak in the anodic scan at around -0.2V with no clear reductive counter-part is the main feature of the CV, while the maximal current achieved was far lower than in turnover conditions. This broad peak is approximately centred at the same potentials as the rising part of the sigmoidal curve in the turnover CV. The peak may be attributable to electroactive cellular components, such as redox proteins or redox mediators (synthetised by the cells), or a mixture of both. The peak is revealing the

approximate redox potential of these species. However, we do not have any further evidence to assign this peak to any specific redox species. There is also a reductive response below -0.3 V. This is probably due to H_2 generation, although the exact nature of this signal is not clear and this phenomenon is still under investigation. For comparison we should mention that in the few reports where the non-turnover CV is shown for microbial anodes on porous structures, the non-turnover CV also features a strong reductive wave.[6, 11]

Figure 4 (thin line) shows the cyclic voltammogram in turnover conditions at the maximum catalytic current for the non-modified RVC electrode. The shape of this CV is very similar to that obtained for biofilm grown on NanoWeb-RVC, except that the current is 2.6 times lower. The similar CV shapes suggest that the electrode material is not affecting the mechanisms and thermodynamics of the microbial catalytic acetate degradation. The plateau current indicates that the maximum current is limited by the enzymatic activity of acetate degradation, and not by the interfacial kinetics of electron transfer. The onset potential for the start of the catalytic sigmoidal signal is governed by the redox potential of the redox moieties (be it soluble shuttles, membrane proteins or nanowires, see discussion below) interacting directly with the electrode surface. Whatever the mechanisms used by bacteria to transfer electrons to the solid electrode, it seems to be the same both in the case of NanoWeb-RVC and unmodified RVC. This is suggested by the similar wave shapes and onset potentials in the two turnover CVs shown in Figure 4.

As seen in Figure 1, both in the SEM images and the photos of both electrodes, the macrostructure of both electrodes is the same, and is only determined by the original mesh density chosen for the departing RVC (45 ppi). Indeed the growth of carbon nanotube NanoWeb is only modifying the RVC surface at the nanoscale. Therefore, we can attribute the significant current difference between the two electrodes to the NanoWeb nanostructured surface morphology. The nanostructured NanoWeb-RVC yields a higher electroactive surface

area, as evidenced in the cyclic voltammogram obtained using a small soluble redox probe, ferricyanide (Figure S3 in Supporting Information). At this point, it should be noted that this increase in surface area does not directly imply more available surface area for bacterial immobilisation. Indeed, the pores created by the NanoWeb are in the nanometre or tenths of nanometre scale, *i.e.* they are at least two orders of magnitude smaller than typical bacterial sizes (about 1 µm length, see Figure 3D). Therefore, we hypothesise that the large current increase in the presence of NanoWeb-RVC is due to an enhanced interaction between the electrode and the microbial cells that boosts the extracellular electron transfer rate. We hypothesise that the texture-style of the CNT NanoWeb is improving the surface's biocompatibility and the interactions of the electroactive bacteria with the electrode surface. By texture, we want to convey the idea of the rather soft nature of the NanoWeb surface in comparison with the bare, fairly flat RVC surface. The NanoWeb surface offers multiple anchorage/contact points for better bacterial adhesion and enhanced electron transfer. The tangled CNT mat in NanoWeb is quite a flexible structure, as opposed to the rigid surface structure of bare RVC.

Extracellular electron transfer can occur through two main mechanisms, direct or mediated electron transfer.[1] For this last option, since we have not added any additional redox mediator, we are referring to mediators synthetized by the bacteria themselves. In regards to direct electron transfer, there are currently two main theories under debate. The first one proposes that redox membrane proteins directly interact with surfaces. The second one postulates that bacteria build up extracellular conductive appendages, also called bacterial nanowires, to electrically interact with surfaces.[1] It is not our objective to determine the more probable electron transfer mechanism, but rather to point out that the texture and flexibility of the NanoWeb structure may facilitate and enhance either of the above mentioned mechanisms.[17] Moreover, in our particular case study, we are working with mixed culture

bacteria and different organisms might transfer electrons via different pathways. The NanoWeb nanostructure makes the electrode surface rough on the nanometre scale, as evidenced in Figures 1C and 1D. For a given bacterium, the NanoWeb electrode will provide more anchoring/contact points and offers much more contact area than the almost atomically flat unmodified RVC.

For the first proposed electron transfer mechanism using membrane redox proteins, it can be expected that there will be an enhancement of the electron transfer rate between membrane redox proteins and the electrode surface. Indeed, bacteria are not rigid organisms, and in the new NanoWeb-RVC electrode, more membrane proteins will approach and be in closer contact with the solid surface. The soft and flexible NanoWeb-RVC will provide an improved interaction between these proteins and the electrode (nanotubes). Particularly, small highly conductive individual carbon nanotubes may come in close contact with membrane proteins and directly electrically interact with them. The distance from the enzyme active centre to the electrode and the nature of the medium through which charge propagates are the main factors governing direct electron transfer.[26] Therefore, if the nanotubes on the electrode surface are closer to the membrane proteins of the microbial cells, the electron transfer rate will be increased. In a similar scenario, for the second proposed electron transfer mechanism via bacterial extracellular appendages, we could expect that these nanometre scale bacterial nanowires might efficiently interact with surface features of analogous dimensions, *i.e.* the flexible carbon nanotubes in the widespread mat formed by the NanoWeb. Finally, for the third proposed electron transfer mechanism using redox mediators, the increased surface area at the nanoscale would play an important role in enhancing the electron collection from small soluble redox mediators excreted by bacteria. Beside the increased surface area also the shorter diffusion distances for the redox molecules will enhance the electron transfer.

Furthermore, the NanoWeb may be trapping these molecules within the active biofilm layer, thereby avoiding losses into the solution.

As stated above, the increase in current density for the NanoWeb-RVC electrode vs. the bare RVC electrode is clearly attributable to the effect of the nanostructure. However, the high current density is also partly attributable to the RVC macrostructure. The catalytic current of (2.3 ± 0.3) mA cm^{-2} measured for the bare RVC electrode indicates that the macrostructure is producing a significant current increase compared to classical flat or merely rough electrodes tested under the same conditions, including same inoculum. For glassy carbon, which presents a similar surface structure as bare RVC, but is a flat electrode, we could only measure (0.45 ± 0.05) mA cm^{-2}. For carbon felt we obtained (1.5 ± 0.1) mA cm^{-2}, in accordance with literature values. [11]

Therefore, considering the new scaffold structure of NanoWeb-RVC as a whole, we believe that our high current density is due to the combined effects of the nanostructure and the macrostructure. The open macrostructure increases the surface area available for microbial loading while at the same time it favours substrate delivery and product diffusion in and out of the three-dimensional structure. It is also important to note that our high current density of 6.8 mA cm^{-2} (normalization to projected surface area) was achieved in room temperature experiments, (20 ± 3)^{o}C. This current value translates into 10.3 mA cm^{-3}. 45 ppi RVC offers a total geometric or real surface area of 26.2 cm^2 cm^{-3} (according to the manufacturer and to Friedrich *et al.*[27]). With this value, we calculate that our NanoWeb-RVC is producing 0.40 mA cm^{-2} (normalization to geometrical or real surface area). On flat rough materials, such as polycrystalline carbon or carbon felt, several authors have reported current densities of 1.0 to 1.6 mA cm^{-2}. Therefore, a value of 0.40 mA cm^{-2} (relative to real surface area, not projected) is around 25-40% of the current density we would expect if all that surface area would be available as a flat electrode. This is a significant advance, even though we believe there is

still room for improvement. This actual surface area-related current is at least one order of magnitude higher than recent reports on novel three-dimensional structures proposed as bioanodes.[13-15, 17]

Several groups in the field of microbial bioelectrochemical systems have tried to take advantage of the great properties of carbon nanotubes, but even in the best situations only achieving around one third of the current compared to the results reported here.[14, 15, 17, 18, 31] In all these cases, the strategy consisted of coating a non-conductive substrate with carbon nanotubes. Instead, our departing structure already showed excellent conductivity and we grew the carbon nanotubes directly onto this substrate by chemical vapour deposition.[30]

To the best of our knowledge, the high current density is only outperformed by the very recent work reported by Schröder *et al.*[6] In that work, the authors reported 7mA cm^{-2} for their basic electrode configuration (less than 5% higher than our work), with further increases from that value as they stack several of the basic electrodes. In work reported here, we have only tested a basic electrode configuration. We are confident that our current density could still improve if we would also stack several of our basic electrodes, although these experiments are still to be done. Moreover, it should again be pointed out that our work was carried out at 20°C, whereas the cited work was performed at 35°C, where bacteria are more active and hence a higher current density could be expected. Finally, at this stage, we have only deposited CNT NanoWeb on RVC of one given porosity (45 ppi). As seen in Figures 1A and 1B, the macropore structure consists of windows or air bubbles of approximately (600 ± 300) µm. Schröder *et al.*[6] presented a macrostructure with windows of between 1.4 and 2.9 mm. Even if this comparison is not strictly valid since their material and electrode design is different from ours, the bioelectrochemical performance of NanoWeb-RVC with even wider openings is expected to be even higher and work in this direction is already under way.

Conclusions

In summary, we have presented a new microbial bioelectrode. This new structure is highly conductive, is cheap and relatively easy to synthetize in large scale. Moreover, the external shape and size of the material can be tailored to any reactor design since the supporting material, RVC, can be cut to the desired shape and size. All these features are of utmost importance as we envisage incorporating these materials into practical devices. Currently bare RVC ($1.50 per cubic inch) would account for 50% of the cost of NanoWeb-RVC, even if this is not the cheapest material proposed to date, the cost is still within reasonable expectations.[8] For scale up beyond certain sizes, there are some limitations with the chemical vapor deposition technique and alternative synthesis protocols are currently being investigated.

Uniform biofilm growth was achieved over the external and internal surface of the three-dimensional scaffold, showing high biocompatibility. The biofilm morphology was very similar both on the outside and the inside of the tree-dimensional scaffold, suggesting that a good mass transport was achieved even deep inside the scaffold.

A very high current density of (6.8 ± 0.3) mA cm^{-2}, (10.3 ± 0.5) mA cm^{-3},was recorded at room temperature with only mild stirring, *i.e.* in the absence of forced flow through the electrode. This high current is attributed to the hierarchical porosity in this unique electrode structure. The macroporous structure hosts a large microbial loading, and at the same time allows good mass transport that supplies substrate needs and removes the undesirable products, mostly H^+ in the current situation. The carbon nanostructure enhances the interaction between the electrode and the microbial biofilm and significantly boosts bacterial extracellular electron transfer.

Experimental

Preparation of NanoWeb materials

The high surface area NanoWeb was grown using chemical vapour deposition (CVD) onto reticulated vitreous carbon (RVC; 45 pores per inch, Duocel, ERG Materials and Aerospace Corporation). The substrate was first coated with a thin layer of catalyst solution consisting of 10% (w/w) iron(III) *para*-toluenesulfonate (Baytron) in ethanol. Substrates were briefly immersed in the 10% (w/w) catalyst solution before being removed, shaken to remove excess solution, and then allowed to dry on laboratory tissue paper until all the excess oxidant had drained from the electrode. The solvent was then removed using a 100 ˚C oven, in which the electrode was subsequently stored.

CVD growth of the NanoWeb material was achieved using a Thermal CVD system (Atomate) that provides computer control over synthesis conditions. Initially the system was flushed with Ar (200 mL min^{-1}) for 30 minutes, after which the furnace temperature was increased to 600˚C whilst a mixture of Ar (150 mL min^{-1}) and H_2 (20 mL min^{-1}) were passed through the furnace. The furnace temperature was then maintained at 600 ˚C for 10 minutes, resulting in reduction of the iron(III) catalyst to iron nanoparticles. Growth of the NanoWeb was then initiated by ramping the temperature up to 800˚C at which point acetylene gas (10 mL min^{-1}) was passed through the furnace whilst maintaining a constant flow of Ar (200 mL min^{-1}) and H_2 (3 mL min^{-1}). Synthesis of the NanoWeb was complete after 30 minutes, at which point the furnace, acetylene and H_2 were turned off, and the system flushed continuously with Ar (150 mL min^{-1}) until the temperature was less than 100 ˚C.

Characterization

Raman was performed on a Jobin Yvon Horiba HR800 confocal Raman microscope using a 632.8nm HeNe laser at a 300 lines/mm grating resolution. Each spectra was taken as an average of 5 scans of 10s each using a 100x wide angle lens. The laser was calibrated against the SiO_2 signal.

Scanning electron microscope (SEM) images were obtained using a JEOL JSM 7500FA cold-field-gun field emission microscope (SEM images shown in Figure 1).

After biofilm development, samples were imaged employing an XL30 Philips (LaB6 source electron gun) Scanning Electron Microscope (SEM images in Figure 3).

Electrochemical activity of RVC with/without NanoWeb modification was characterized using eDAQ EChem system to carry out cyclic voltammograms in a standard three-electrode cell with a 0.1M $NaNO_3$ solution containing 10mM ferricyanide at a scan rate of 5 mV s^{-1}.

Electrode preparation

Both NanoWeb-RVC and unmodified RVC were pierced with a 0.5mm thick Ti wire that acted as a current collector. The electrical connection was reinforced by means of conductive C paint that was let to dry for 3 days. Electrodes were cut in blocks of around (1 x 1) cm, and they were 0.66cm thick.

The projected surface area of the electrodes refers to the fingerprint of the base of the electrode; i.e. for an electrode that is a block of (1 x 1) cm and 0.66 cm thick, the projected surface area would be 1 cm^2. The projected surface area of two pieces of same external geometry of NanoWeb-RVC and bare-RVC is therefore the same.

The geometrical or real surface area refers to the total surface area of the RVC scaffold before NanoWeb deposition (*i.e.* the geometrical surface area is the same for bare RVC and for NanoWeb-RVC). For a 45ppi RVC a value is 26.2 cm^2 cm^{-3} is informed by the RVC manufacturer and is confirmed by Friedrich *et al.*[27]

Electrodes (both NanoWeb-RVC and RVC) were pre-treated in a N_2 plasma for 15 minutes before being introduced in the reactor.

Since the carbon paint blocked a few of the pores, the surface area and the volume values used for normalization of current densities do not consider this area/volume.

Bioelectrochemical experiments

All bioelectrochemical experiments were carried out under strictly anoxic conditions (all solutions were bubbled with N_2 gas for 30 minutes) and under potentiostatic control. All the electrodes were tested in a membraneless home-made electrochemical reactor (600 mL). A home-made Ag/AgCl (saturated Cl^-) reference electrode was used and all potentials reported here are referred to this electrode. A large area Ti mesh was used as a counter electrode. All potentials in this manuscript are referred to the Ag/AgCl (saturated Cl^-) reference electrode. All experiments were performed in duplicate. Maximum current values for duplicate experiments were always within 10%.

A Biologic VSP multichannel potentiostat was used for all experiments. The electrode was introduced in the bioelectrochemical reactor in a solution of M9 medium (see below) without acetate. The background signal both for chronoamperometry and CV experiments was measured prior to inoculation. After measuring the background, the reactor was inoculated with 200ml of anodic effluent of an existing bioelectrochemical reactor in our laboratory at The University of Queensland.[33] Acetate was added to a final concentration of 20mM. After inoculation, no potential was applied during 24h, then the electrodes were connected and a constant potential of 0V was applied for the total duration of the experiments. From the start of the experiment, a magnetic stirrer was used to mix the solution at a rotation rate of 100 RPM, this rotation rate was increased as indicated in the text. The medium used was a modified M9 medium with 20 mM sodium acetate as the electron donor, which contains 6 g/ L Na_2HPO_4, 3 g/L KH_2PO_4, 0.1 g/L NH_4Cl, 0.5 g/L NaCl, 0.1 g/ L $MgSO_4 \cdot 7H_2O$, 14.6 mg/ L $CaCl_2$, and 1 mL/L of a mixed trace element solution as described in Rabaey *et al*.[34]

CORRESPONDING AUTHOR

*corresponding author: Victoria Flexer

v.flexer@awmc.uq.edu.au

T +61 7 3346 72 11

F +61 7 3365 4726

ACKNOWLEDGMENTS

VF acknowledges a UQ Postdoctoral Fellowship. This work was supported by the Australian Research Council Grants DP0985317 and DP110100539. JC and GGW would like to thank the ACES and ANFF for continuous support. In addition, GGW acknowledges the support of the ARC in the form of an Australian Laureate Fellowship. The authors acknowledge the facilities and the scientific and technical assistance of the Australian Microscopy & Microanalysis Research Facility at the Centre for Microscopy and Microanalysis (The University of Queensland). The authors thank Dr B. Virdis for fruitful discussions.

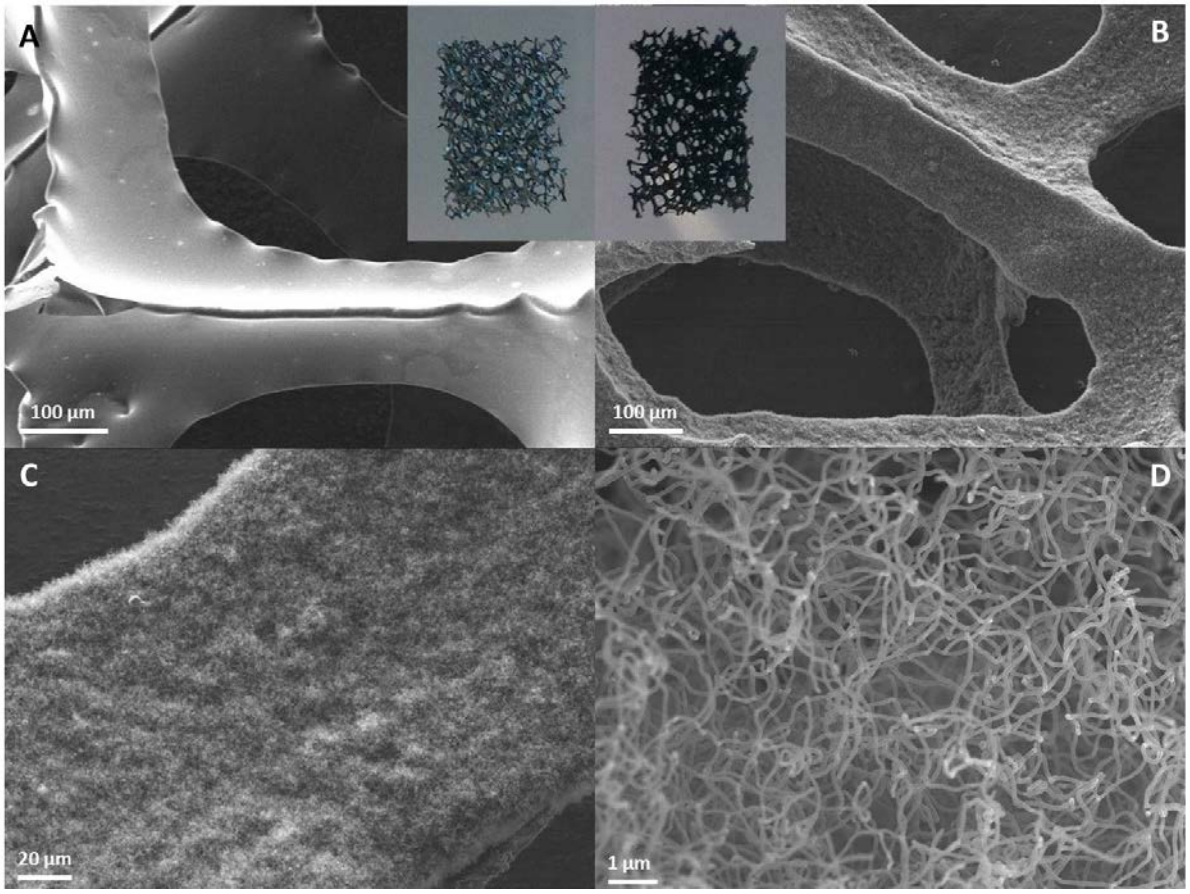

Figure 1: Scanning Electron Micrographs (SEM) images of (A) Unmodified reticulated vitreous carbon, RVC; (B), (C), and (D) Carbon NanoWeb deposited onto RVC (NanoWeb-RVC) at different magnifications. Insets in (A) and (B) are photographic images of unmodified RVC, and NanoWeb deposited onto RVC, respectively. The NanoWeb structure was grown by modifying the generally employed route of chemical vapour deposition (CVD).

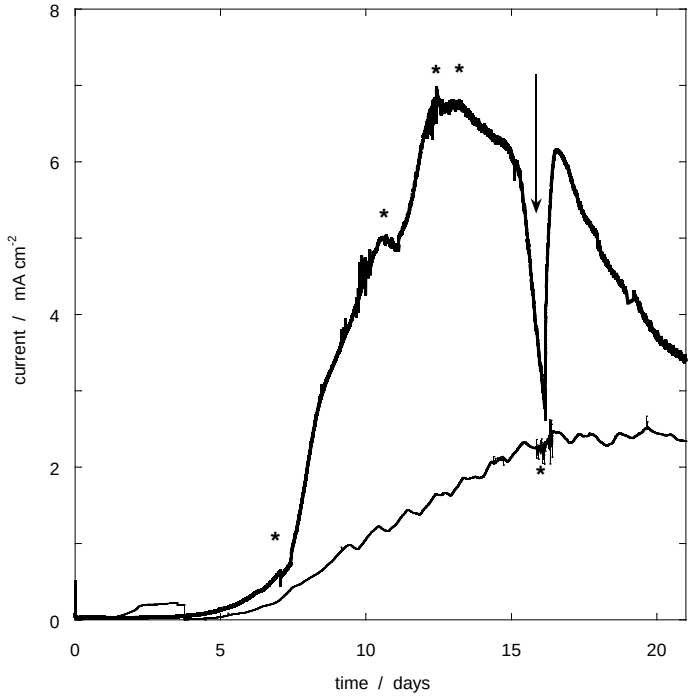

Figure 2: Bioelectrocatalytic current generation at a NanoWeb-RVC electrode (thick line) and bare RVC electrode (thin line) in batch experiments. Biofilms derived from an anodic effluent and grown in artificial wastewater with 20 mM acetate. The applied electrode potential was 0 V (vs. Ag/AgCl) and the experiment was performed at room temperature (20 ± 3) ^{o}C. The arrow indicates new substrate feed. The asterisks mark time points when the stirring speed was changed (see details in text).

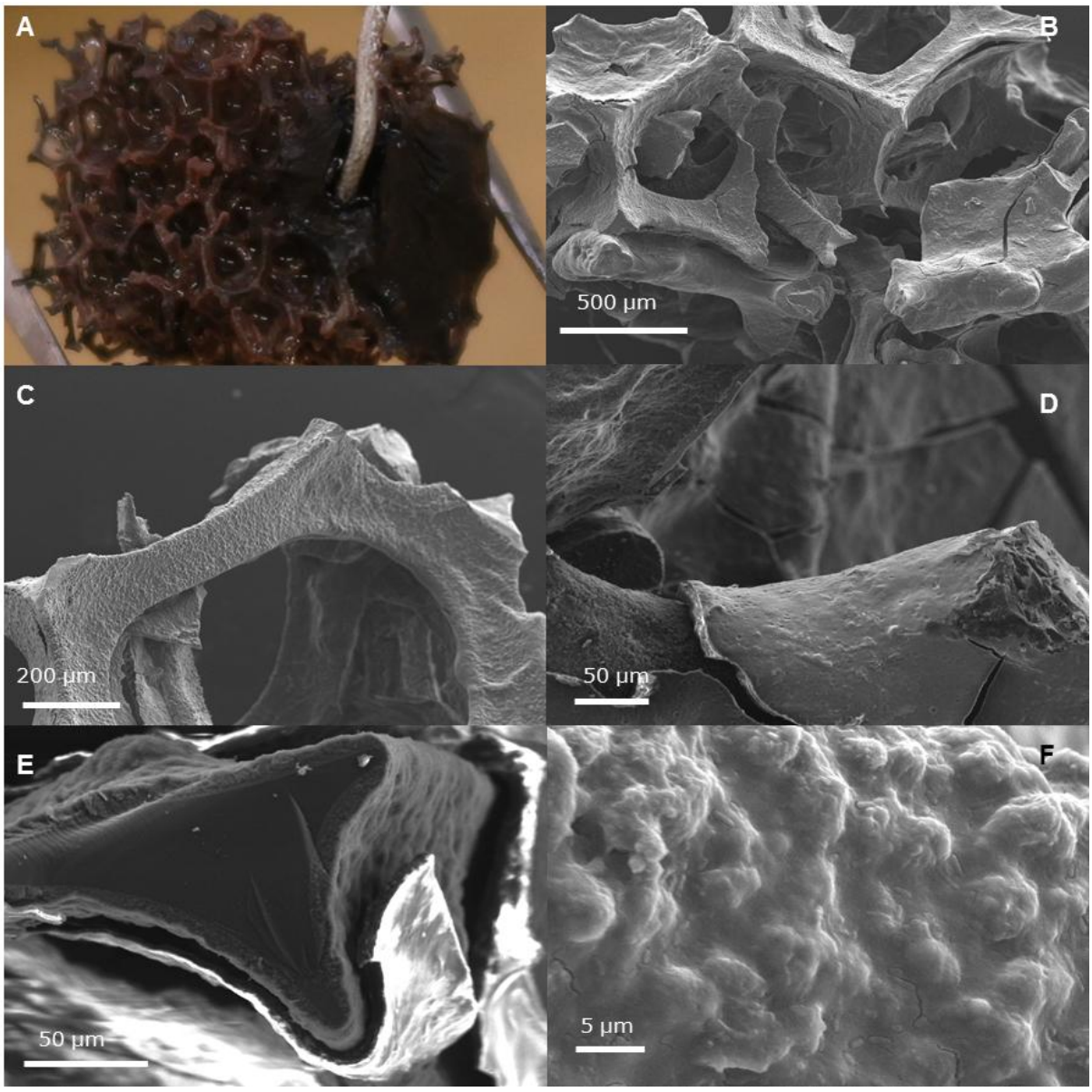

Figure 3: (A) NanoWeb-RVC electrode after biofilm growth. Note the reddish colour of the biofilm. The Ti wire current collector can also be seen. (B) to (F) SEM images of an electroactive biofilm grown on NanoWeb-RVC at different magnifications. The scaffold was fractured to show the features of interest.

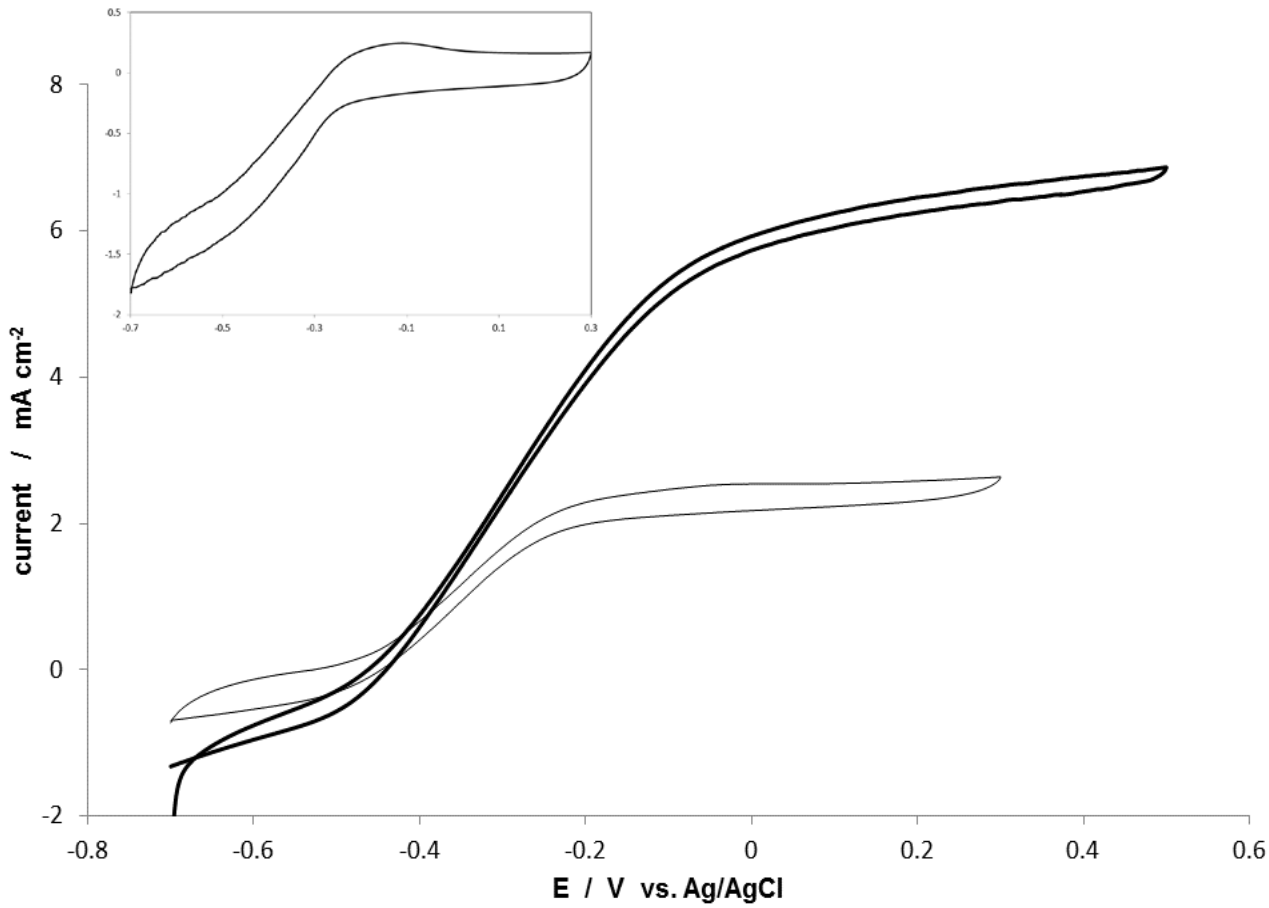

Figure 4: Cyclic voltammogram of electroactive biofilms in turnover conditions grown on NanoWeb-RVC electrode (thick line) and unmodified RVC electrode (thin line). Inset: Cyclic voltammogram of NanoWeb-RVC electrode in the absence of acetate (non-turnover conditions, note different y-axis scale). Scan rate $1mVs^{-1}$. Biofilms derived from an anodic effluent and grown in artificial wastewater with 20 mM acetate. The applied electrode potential was 0 V (vs. Ag/AgCl) and the experiment was performed at room temperature. All other conditions are the same as in Figure 2.

References

1. *Bioelectrochemical Systems: From Extracellular Electron Trnasfer to Biotechnological Applications*, IWA Publishing, London, 2010.
2. B. E. Logan, *Nature Reviews Microbiology*, 2009, **7**, 375-381.
3. D. R. Lovley, *Nature Reviews Microbiology*, 2006, **4**, 497-508.
4. K. Rabaey and W. Verstraete, *Trends in Biotechnology*, 2005, **23**, 291-298.
5. K. Rabaey and R. A. Rozendal, *Nature Reviews Microbiology*, 2010, **8**, 706-716.
6. S. Chen, G. He, Q. Liu, F. Harnisch, Y. Zhou, Y. Chen, H. Muddasir, S. Wang, X. Peng, H. Hou and U. Schroeder, *Energy & Environmental Science*, 2012, **5**, 9769-9772.
7. B. E. Logan, *Applied Microbiology and Biotechnology*, 2010, **85**, 1665-1671.
8. R. A. Rozendal, H. V. M. Hamelers, K. Rabaey, J. Keller and C. J. N. Buisman, *Trends in Biotechnology*, 2008, **26**, 450-459.
9. M. Zhou, M. Chi, J. Luo, H. He and T. Jin, *Journal of Power Sources*, 2011, **196**, 4427-4435.
10. J. Wei, P. Liang and X. Huang, *Bioresource Technology*, 2011, **102**, 9335-9344.
11. S. Chen, H. Hou, F. Harnisch, S. A. Patil, A. A. Carmona-Martinez, S. Agarwal, Y. Zhang, S. Sinha-Ray, A. L. Yarin, A. Greiner and U. Schroder, *Energy & Environmental Science*, 2011, **4**, 1417-1421.
12. S. Chen, Q. Liu, G. He, Y. Zhou, M. Hanif, X. Peng, S. Wang and H. Hou, *Journal of Materials Chemistry*, 2012, **22**, 18609-18613.
13. Z. He, J. Liu, Y. Qiao, C. M. Li and T. T. Y. Tan, *Nano Letters*, 2012, **12**, 4738-4741.
14. S. R. Higgins, D. Foerster, A. Cheung, C. Lau, O. Bretschger, S. D. Minteer, K. Nealson, P. Atanassov and M. J. Cooney, *Enzyme and Microbial Technology*, 2011, **48**, 458-465.
15. K. Katuri, M. L. Ferrer, M. C. Gutiérrez, R. Jiménez, F. Del Monte and D. Leech, *Energy and Environmental Science*, 2011, **4**, 4201-4210.
16. J. E. Mink, J. P. Rojas, B. E. Logan and M. M. Hussain, *Nano Letters*, 2012, **12**, 791-795.
17. X. Xie, L. Hu, M. Pasta, G. F. Wells, D. Kong, C. S. Criddle and Y. Cui, *Nano Letters*, 2011, **11**, 291-296.
18. X. Xie, M. Ye, L. Hu, N. Liu, J. R. McDonough, W. Chen, H. N. Alshareef, C. S. Criddle and Y. Cui, *Energy & Environmental Science*, 2012, **5**, 5265-5270.
19. S. Chen, G. He, A. A. Carmona-Martinez, S. Agarwal, A. Greiner, H. Hou and U. Schröder, *Electrochemistry Communications*, 2011, **13**, 1026-1029.
20. Y. Zhao, K. Watanabe, R. Nakamura, S. Mori, H. Liu, K. Ishii and K. Hashimoto, *Chemistry - A European Journal*, 2010, **16**, 4982-4985.
21. S. Chen, G. He, X. Hu, M. Xie, S. Wang, D. Zeng, H. Hou and U. Schröder, *ChemSusChem*, 2012, **5**, 1059-1063.
22. A. E. Franks, K. P. Nevin, H. Jia, M. Izallalen, T. L. Woodard and D. R. Lovley, *Energy and Environmental Science*, 2009, **2**, 113-119.
23. U. Schröder, *Physical Chemistry Chemical Physics*, 2007, **9**, 2619-2629.
24. C. I. Torres, A. K. Marcus and B. E. Rittmann, *Biotechnology and Bioengineering*, 2008, **100**, 872-881.
25. V. Flexer, N. Brun, R. Backov and N. Mano, *Energy and Environmental Science*, 2010, **3**, 1302-1306.
26. V. Flexer, N. Brun, O. Courjean, R. Backov and N. Mano, *Energy and Environmental Science*, 2011, **4**, 2097-2106.
27. J. M. Friedrich, C. Ponce-de-León, G. W. Reade and F. C. Walsh, *Journal of Electroanalytical Chemistry*, 2004, **561**, 203-217.

28. Z. He, S. D. Minteer and L. T. Angenent, *Environmental Science and Technology*, 2005, **39**, 5262-5267.
29. B. R. Ringeisen, E. Henderson, P. K. Wu, J. Pietron, R. Ray, B. Little, J. C. Biffinger and J. M. Jones-Meehan, *Environmental Science & Technology*, 2006, **40**, 2629-2634.
30. J. Chen, A. I. Minett, Y. Liu, C. Lynam, P. Sherrell, C. Wang and G. G. Wallace, *Advanced Materials*, 2008, **20**, 566-570.
31. M. C. Gutierrez, Z. Y. Garcia-Carvajal, M. J. Hortiguela, L. Yuste, F. Rojo, M. L. Ferrer and F. del Monte, *Journal of Materials Chemistry*, 2007, **17**, 2992-2995.
32. S. J. Little, S. F. Ralph, N. Mano, J. Chen and G. G. Wallace, *Chemical Communications*, 2011, **47**, 8886-8888.
33. P. G. Dennis, K. Guo, M. Imelfort, P. Jensen, G. W. Tyson and K. Rabaey, *Bioresource Technology*, 2013, **129**, 599-605.
34. K. Rabaey, W. Ossieur, M. Verhaege and W. Verstraete, *Water Science and Technology*, 2005, **52**, 515-523.

TABLE OF CONTENTS/GRAPHICAL ABSTRACT

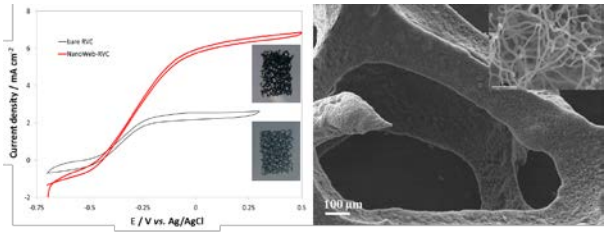

Very high current densities are developed when a microbial biofilm is developed in this new material. The NanoWeb-RVC scaffold combines the advantages of open macrostructure and the carbon nanotube nanostructure.

BROADER CONTEXT PARAGRAPH

In microbial bioelectrochemical systems, whole cells are used as biocatalysts to catalyse oxidation and/or reduction reactions. The concept is very promising, with many prospective advantages, particularly with regards to the use of self-(re)generating and inexpensive catalysts, and operation under mild conditions (room temperature and ambient pressure).

Microbial fuel cells are the classical example of bioelectrochemical systems, performing the double task of wastewater treatment (*i.e.* using waste as fuel) and electricity generation. The viability and industrial application of such systems is highly dependent on improved performance, particularly in terms of higher currents for a given reactor size. The electrode materials are at the centre of the current generation limitations and until very recently, most of the work on bioelectrochemical systems used only commercially available materials. The purpose-specific design and synthesis of new electrode materials for such microbial electrochemical processes has only started recently.

We have synthesized a new microbial electrode material using a hierarchical porous structure, NanoWeb-RVC, where carbon nanotubes were directly grown on a macroporous highly conductive scaffold. Results show that the new material combines the advantages of the nanostructure to enhance the extracellular electron transfer with the open macrostructure that achieves effective mass transfer into the entire three-dimensional scaffold.